Crystal Structures of Potassium Tetratellurite, $K_2Te_4O_9$, and Potassium Ditellurite, $K_2Te_2O_5$, and Structural Trends in Solid Alkali Tellurites

C. R. Becker, S. L. Tagg, J. C. Huffman, and J. W. Zwanziger*

Department of Chemistry and Molecular Structure Center, Indiana University, Bloomington, Indiana 47405

Received April 29, 1997[⊗]

The crystal structures of potassium tetratellurite and potassium ditellurite are reported, completing the series of known phases of alkali tellurites including lithium, sodium, potassium and cesium. Potassium tetratellurite ($K_2Te_4O_9$, $a = 7.572(1)$ Å, $b = 17.821(3)$ Å, $c = 7.829(1)$ Å, $\beta = 108.62°$, monoclinic, $P2_1/c$, $Z = 4$) contains linked 12-membered tellurite rings, coordinated by potassium. The ditellurite ($K_2Te_2O_5$, $a = 5.454(1)$ Å, $b = 15.142(1)$ Å, $c = 7.731(1)$ Å, $\beta = 93.71(1)°$, $Z = 4$), monoclinic, $P2_1/a$, $Z = 4$) consists of infinite chains separated by rough sheets of cations. Comparison of the different alkali tellurite structures confirms the qualitative picture that as alkali oxide is added, the tellurite network is increasingly cleaved. We show, however, that the extent of network cleavage depends significantly on the nature of the modifying ion, with lithium inducing the fewest nonbridging oxygens per equivalent and potassium and cesium inducing as many as two nonbridging oxygens per equivalent of added cation. This behavior is due to the stability in tellurites of delocalized electrons across several nonbridging oxygens and is contrasted with the much simpler and well-known case of silicate modification.

Introduction

Glasses based on tellurite (TeO_2) show strikingly high nonlinear-optical susceptibility,[1] and also anomalous glass-forming behavior.[2] In particular, while TeO_2 itself is only a conditional glass former, alkali tellurites ($(M_2O)_x(TeO_2)_{1-x}$, M = Li, Na, K) form stable glasses easily with x in the range from 10 to 25 mol % and even to 35 mol % in the case of sodium. The structures of these glasses have been studied intensively over the last several years, but a consensus has not emerged.[3−9] The primary reason for this difficulty is the richness of tellurite chemistry, as compared to the lighter main-group oxides typically used as glass formers, in particular SiO_2 and P_2O_5 and to a lesser extent B_2O_3.

When 1 equiv of an alkali oxide modifier (M_2O) is added to a glass, the expectation is that 2 equiv of nonbridging oxygen (NBO) will be formed, as shown in Scheme 1.[10] The result is that the glass network is partially cleaved by the modifier, which results in a lower average coordination number and, hence, a weaker network, and a lower glass-transition temperature. This expectation works well for silicate chemistry, but fails when there are several possible sources of charge compensation for the added M^+ ions. Thus, in borate glasses, Scheme 1 does not prevail until 30% or more M_2O is added; at lower concentrations, three-coordinate boron atoms of B_2O_3 are converted to tetrahedral, four-coordinate species $BO_{4/2}^-$. The consequences of this type of modification in glass manufacture are significant, because creation of $BO_{4/2}^-$ leads to a higher average coordination number (CN) and an increase in the glass-transition temperature, in contrast to the usual effect of modifiers.

Scheme 1

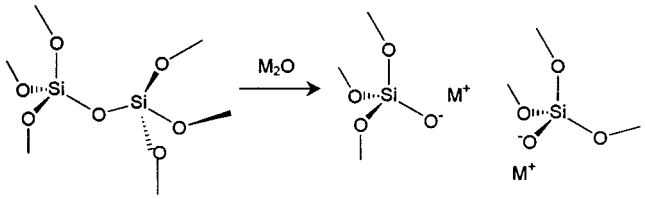

The difficulty in identifying the structural changes in tellurite glasses upon addition of alkali oxide modifiers is also due to the variety of possible sources of charge compensating species. This circumstance arises from the charge delocalization that commonly occurs in oxygen−tellurium bonds. For example, tellurite itself consists of $TeO_{4/2}$ units,[11,12] while M_2TeO_3 (M = Li, Na, K, Cs) consists of individual TeO_3^{2-} ions (Figure 1) coordinated by alkali cations.[13−15] Chemically, M_2TeO_3 can be viewed as TeO_2 modified by 50 mol % of M_2O, and here it is seen that rather than forming one NBO (nonbridging oxygen) per added modifier ion, 1.5 NBOs are created (3 NBOs per 2 M^+). In tellurite glasses formed with less than 50% M_2O, a variety of structures, such as $TeO_{3/2}O^-$, $TeO_{1/2}O_2^-$, and so forth have been postulated (Figure 1).[6,7,9] To evaluate the likelihood of these structures in glasses, it is helpful to consider crystal phases of similar composition. These are known to exist at

[⊗] Abstract published in *Advance ACS Abstracts,* October 15, 1997.

(1) El-Mallawany, R. *J. Appl. Phys.* **1992**, *72*, 1774.
(2) Heo, J.; Lam, D.; Sigel, G. H., Jr.; Mendoza, E. A.; Hensley, D. A. *J. Am. Ceram. Soc.* **1992**, *75*, 277.
(3) Neov, S.; Kozhukharov, V.; Gerasimova, I.; Krezhov, K.; Sidzhimov, B. *J. Phys. C* **1979**, *12*, 2475.
(4) Yoko, T.; Fujita, M.; Miyaji, F.; Sakka, S. *Chem. Express* **1990**, *5*, 549.
(5) Kowada, Y.; Habu, K.; Adachi, H.; Tatsumisago, M.; Minami, T. *Chem. Express* **1992**, *7*, 965.
(6) Sekiya, T.; Mochida, N.; Ohtsuka, A.; Tonokawa, M. *J. Non-Cryst. Solids*. **1992**, *144*, 128.
(7) Tatsumisago, M.; Minami, T.; Kowada, Y.; Adachi, H. *Phys. Chem. Glasses.* **1994**, *35*, 89.
(8) Tagg, S. L.; Youngman, R. E.; Zwanziger, J. W. *J. Phys. Chem.* **1995**, *99*, 511.
(9) Uchino, T; Yoko, T. *J. Non-Cryst. Solids* **1996**, *204*, 243.
(10) Varshneya, A. K. *Fundamentals of Inorganic Glasses*; Academic Press: San Diego, CA, 1994.
(11) Lindqvist, O. *Acta Chem. Scand*. **1968**, *22*, 977.
(12) Beyer, H. *Z. Kristallogr*. **1967**, *124*, 228.
(13) Folger, F. *Z. Anorg. Allg. Chem*. **1975**, *411*, 103.
(14) Masse, R.; Guitel, J. C.; Tordjman, I. *Mater. Res. Bull*. **1980**, *15*, 431.
(15) Andersen, L.; Langer, V.; Strömberg, A.; Strömberg, D. *Acta Crystallogr*. **1989**, *B45*, 344.

S0020-1669(97)00497-7 CCC: $14.00

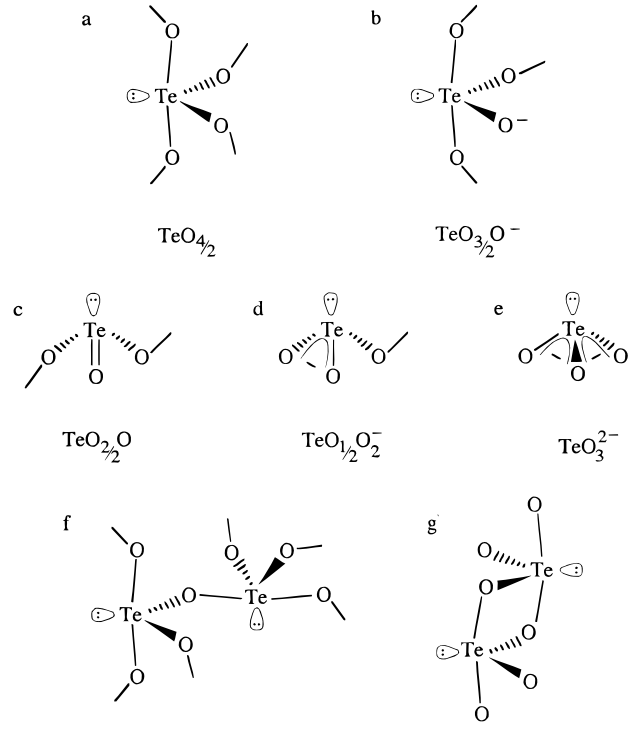

Figure 1. Structures found in tellurites. (a) the basic trigonal bipyramidal unit, with the lone pair occupying one of the equatorial sites. (b−e) Tellurite units with nonbridging oxygen. The NBO can carry a charge of 1, as in b, but can also be neutral, as in c, or several NBOs can share units of charge, as in d and e. (f and g) How the basic units are linked, with either one oxygen corner-shared, as in f, or two oxygens edge-shared, as in g. Axial sites on one group are bonded to equatorial sites on the linked group, and vice versa.

20% M_2O for M = Na , K, and Cs and at 33% M_2O for Li, Na, K, and Cs.[16,17] The Li- and Cs-based structures have been determined previously.[17,18] Recently, we succeeded in solving both Na structures.[19,20]

The purpose of this paper is to report the structures of both $K_2Te_4O_9$ and $K_2Te_2O_5$, the potassium-modified tellurites with 20% and 33% modifier, respectively. Additionally, we make detailed structural comparisons of the entire series of alkali-oxide-modified tellurite crystals. We find that, as expected from the 50% modification, the number of NBOs exceeds the number of added modifier ions, due to charge delocalization in the tellurium oxide fragments. However, this effect is rather strongly cation-dependent: it is maximized for potassium and cesium and minimized for lithium. We conjecture that this is the result of steric hindrance coupled with Coulombic repulsion: bulky charged groups, tethered to the tellurite network, are energetically too costly to pack around a small lithium ion, while they can be accommodated much more easily around the large potassium and cesium ions.

The outline of the paper is as follows: in the next section we describe the preparation of the potassium tellurite crystals and the crystallographic methods used to solve the structures. We then present details of the new structures and also a detailed comparison with the Li, Na, and Cs tellurite structures. We finish with conclusions on both the crystal chemistry and its significance for tellurite glasses.

(16) Tellur, In *Gmelin Handbook of Inorganic Chemistry*; Hantke, G., Ed.; Springer-Verlag: Berlin, Germany, 1976.
(17) Loopstra, B. O.; Goubitz, K. *Acta Crystallogr*. **1986**, *C42*, 520.
(18) Cachau-Herreillat, D.; Norbert, A.; Maurin, M.; Philippot, E. *J. Solid State Chem*. **1981**, *37*, 352.
(19) Tagg, S. L.; Huffman, J. C.; Zwanziger, J. W. *Chem. Mater*. **1994**, *6*, 1884.
(20) Tagg, S. L.; Huffman, J. C.; Zwanziger, J. W. *Acta Chem. Scand*. **1997**, *51*, 118.

Table 1. Data Collection and Refinement Parameters for Crystal Structure Determinations

	$K_2Te_4O_9$	$K_2Te_2O_5$
mol wt	732.59	413.39
space group	$P2_1/c$ (No. 14)	$P2_1/a$ (No. 14)
a (Å)	7.572(1)	5.454(1)
b (Å)	17.821(3)	15.142(1)
c (Å)	7.829(1)	7.713(1)
β (deg)	108.62(1)	93.71(1)
V (Å^3)	1001.08	635.62
Z (molecules/cell)	4	4
ρ (g/cm^3)	4.861	4.320
linear abs coeff (cm^{-1})	124.372	104.657
temp (°C)	−169	−170
Mo Kα, λ (Å)	0.71069	0.71069
$R_w(F_o)^a$	0.0281	0.0213
$R(F_o)^a$	0.0281	0.0206

[a] R factors calculated as $R = (\sum||F_o| - |F_c||)/\sum|F_o|$, $R_w = (\sum w||F_o| - |F_c||)/\sum w|F_o|$.

Experimental Section

Crystal Growth. Crystals of both $K_2Te_2O_5$ and $K_2Te_4O_9$ were prepared from melts. Stoichiometric amounts of K_2CO_3 (Aldrich, 99.99%) and TeO_2 (Alfa, 99.995%) were well mixed and heated in a silica glass tube at 780 °C for roughly 10 min, allowing rapid evolution of CO_2. The molten samples were immediately quenched over stainless steel. Subsequent heat treatment of the resulting amorphous solids differed for the two compositions. $K_2Te_4O_9$ (mp 485 °C, ref 16) was placed in a silica glass boat in a 500 °C furnace and then cooled at a rate of 1 °C/min for 1 h. The sample was left at 460 °C for 16 h, followed by cooling to room temperature at a rate of 0.8 °C/min. $K_2Te_2O_5$ (mp 510 °C, ref 16) was heated in a platinum crucible at 540 °C for 20 min before cooling to room temperature at a rate of 0.2 °C/min. It was then recrystallized in the same crucible at 540 °C for 20 min before cooling to room temperature at a rate of 2.0 °C/min.

Structure Determination. Small fragments of the resulting crystals were cleaved from the larger masses of crystals and attached to the ends of glass fibers using silicone grease. $K_2Te_4O_9$ was ground into a sphere of diameter 0.18 mm to simplify absorption corrections. The crystals were transferred to a goniostat, where they were cooled to −170 °C for characterization and data collection. Systematic searches of a limited hemisphere of reciprocal space located a set of diffraction maxima with systematic absences and symmetry corresponding to the monoclinic space group $P2_1/c$ for $K_2Te_4O_9$ and the monoclinic space group $P2_1/a$ for $K_2Te_2O_5$. Subsequent solution and refinement confirmed these choices.

The data were collected using a standard moving crystal, moving detector technique with fixed backgrounds at each extreme of the scan. Data were corrected for Lorentz and polarization effects, and equivalent reflections were averaged. Corrections were made for the presence of extinction. The structures were readily solved by direct methods (MULTAN78) and Fourier techniques. The final Fourier difference maps were essentially featureless.

Results of Crystallography

Experimental details of the crystallography are provided in Table 1. Fractional coordinates and thermal parameters of the crystals are provided in Table 2. Selected bond lengths and angles for $K_2Te_4O_9$ are listed in Tables 3 and 4, respectively, and for $K_2Te_2O_5$, in Tables 5 and 6. Figure 2 shows two unit cells of $K_2Te_4O_9$ illustrating the tellurite sheets separated by cations, and Figure 3 shows the asymmetric unit and its connectivity to the rest of the structure. Figure 4 shows the tellurite chains in $K_2Te_2O_5$ separated by rough sheets of cations. The asymmetric unit and its connectivity are shown in Figure 5.

Table 2. Fractional Coordinates and Isotropic Thermal Parameters U_{iso} for $K_2Te_4O_9$ and $K_2Te_2O_5$

atom	*x*	*y*	*z*	U_{iso} (Å^2)
		$K_2Te_4O_9$		
Te(1)	0.3947(1)	0.41639(3)	0.4051(1)	0.00533(17)
Te(2)	0.8313(1)	0.41151(4)	0.3360(1)	0.00590(17)
Te(3)	0.3633(1)	0.42160(4)	0.8498(1)	0.00617(17)
Te(4)	0.6209(1)	0.24056(3)	0.5495(1)	0.00550(17)
K(1)	0.1555(3)	0.2554(1)	0.6223(3)	0.0087(6)
K(2)	0.8812(3)	0.4088(1)	0.8689(3)	0.0113(6)
O(1)	0.6079(9)	0.4440(4)	0.5871(9)	0.0080(19)
O(2)	0.4095(10)	0.3083(4)	0.4172(9)	0.0077(19)
O(3)	0.1620(10)	0.5055(4)	0.8256(9)	0.0107(23)
O(4)	0.2561(9)	0.4089(4)	0.5932(9)	0.0100(21)
O(5)	0.8840(10)	0.3417(4)	0.1835(9)	0.0120(23)
O(6)	0.5669(9)	0.4110(4)	0.2382(9)	0.0093(19)
O(7)	0.2199(10)	0.3543(4)	0.9201(9)	0.0107(23)
O(8)	0.5578(10)	0.3254(4)	0.8503(9)	0.0093(21)
O(9)	0.7989(10)	0.2993(4)	0.5004(9)	0.0107(23)
		$K_2Te_2O_5$		
Te(1)	0.2521(1)	0.06303(3)	0.1216(1)	0.00690(17)
Te(2)	0.7018(1)	0.18351(3)	0.4162(1)	0.00663(17)
K(1)	0.7658(3)	0.1815(1)	−0.1190(2)	0.0103(6)
K(2)	0.2366(3)	0.0674(1)	0.6277(2)	0.0093(11)
O(1)	0.7357(9)	0.0896(3)	0.5660(6)	0.0103(17)
O(2)	1.0033(9)	0.2442(3)	0.5548(6)	0.0097(17)
O(3)	−0.0846(9)	0.0625(3)	0.1455(7)	0.0140(17)
O(4)	0.3416(9)	0.1366(3)	0.3174(6)	0.0107(17)
O(5)	0.2774(9)	0.1458(3)	−0.0522(6)	0.0113(17)

Table 3. Selected Bond Lengths (Å) in $K_2Te_4O_9$

Te(1)−Te(1^a)	3.4811(6)	Te(3)−K(1)	3.5532(9)
Te(1)−Te(2)	3.5171(11)	Te(3)−K(2^g)	3.7078(24)
Te(1)−Te(3)	3.5659(8)	Te(4)−K(1)	3.7546(25)
Te(1)−Te(4)	3.5768(6)	K(1)−O(7^b)	2.658(4)
Te(2)−Te(3^a)	3.4297(5)	K(1)−O(9^g)	2.677(7)
Te(2)−Te(4^b)	3.5540(5)	K(1)−O(2^c)	2.735(4)
Te(3)−Te(4^c)	3.5572(6)	K(1)−O(7)	2.8374(26)
Te(1)−O(1)	1.846(5)	K(1)−O(5^h)	2.843(6)
Te(1)−O(2)	1.9307(4)	K(1)−O(4)	2.8670(23)
Te(1)−O(4)	2.068(6)	K(1)−O(2)	3.023(7)
Te(1)−O(6)	2.122(6)	K(1)−O(8^c)	3.247(6)
Te(1)−O(1^a)	2.4890(4)	K (6)−O(1)	2.574(4)
Te(2)−O(5)	1.853(4)	K (6)−O(7^d)	2.651(7)
Te(2)−O(6)	1.902(7)	K (6)−O(5^e)	2.731(4)
Te(2)−O(3)	1.9575(26)	K (6)−O(8^c)	2.829(7)
Te(2)−O(9)	2.4326(26)	K (6)−O(3^f)	2.840(6)
Te(3)−O(7)	1.816(5)	K (6)−O(3^e)	2.942(4)
Te(3)−O(4)	1.925(3)	K (6)−O(9)	3.373(3)
Te(3)−O(3^a)	2.100(5)	O(1)−O(1^a)	2.663(7)
Te(3)−O(8^c)	2.260(5)	O(1)−O(6)	2.713(5)
Te(4)−O(9)	1.842(6)	O(1)−O(4)	2.751(10)
Te(4)−O(8)	1.8886(22)	O(2)−O(4)	2.736(7)
Te(4) -O(2)	2.008(5)	O(2)−O(8)	2.754(5)
Te(4)−O(5^c)	2.426(5)	O(2)−O(6)	2.792(7)
K(1)−K(2^i)	3.7664(14)	O(3)−O(6)	2.708(8)
K(1)−K(1^c)	3.9191(7)	O(3)−O(5)	2.7434(13)
K(2)−K(2^j)	3.9564(16)	O(3)−O(4^a)	2.759(6)
Te(2)−K(2^k)	3.7946(16)	O(3)−O(7^a)	2.7905(13)

^{a} $\bar{x}+1, \bar{y}+1, \bar{z}+1$. ^{b} $x, \bar{y}+1/2, z-1/2$. ^{c} $x, \bar{y}+1/2, z+1/2$. ^{d} $x+1, y, z$. ^{e} $x, y, z+1$. ^{f} $\bar{x}+2, \bar{y}+1, \bar{z}+1$. ^{g} $x-1, y, z$. ^{h} $x-1, \bar{y}+1/2, z+1/2$. ^{i} $x-1, \bar{y}+1/2, z-1/2$. ^{j} $\bar{x}+2, \bar{y}+1, \bar{z}+2$. ^{k} $x, y, z-1$.

Table 4. Selected Bond Angles (deg) in $K_2Te_4O_9$

O(1)−Te(1)−O(2)	101.84(15)	O(9)−Te(4)−O(5^c)	83.04(19)
O(1)−Te(1)−O(4)	89.14(23)	O(8)−Te(4)−O(2)	89.88(16)
O(1)−Te(1)−O(6)	85.98(22)	O(8)−Te(4)−O(5^c)	86.40(17)
O(1)−Te(1)−O(1^a)	74.13(16)	O(2)−Te(4)−O(5^c)	174.59(19)
O(2)−Te(1)−O(4)	86.26(18)	O(7^b)−K(1)−O(9^g)	111.01(15)
O(2)−Te(1)−O(6)	86.98(19)	O(7^b)−K(1)−O(2^c)	89.08(11)
O(5)−Te(2)−O(6)	98.78(22)	O(7^b)−K(1)−O(7)	158.49(24)
O(5)−Te(2)−O(3)	92.01(14)	O(7^b)−K(1)−O(5^h)	86.11(15)
O(5)−Te(2)−O(9)	82.42(14)	O(1)−K(2)−O(7^d)	133.87(16)
O(6)−Te(2)−O(3)	89.13(22)	O(1)−K(2)−O(5^e)	130.68(22)
O(6)−Te(2)−O(9)	86.42(17)	O(1)−K(2)−O(8^c)	68.77(14)
O(3)−Te(2)−O(9)	172.26(12)	O(7)−K(2)−O(5^f)	88.57(17)
O(7)−Te(3)−O(4)	98.33(18)	Te(1)−O(1)−Te(1^a)	105.88(16)
O(7)−Te(3)−O(3^a)	90.60(22)	Te(1)−O(2)−Te(4)	130.5(3)
O(7)−Te(3)−O(8^c)	87.19(22)	Te(2)−O(3)−Te(3^a)	115.4(3)
O(4)−Te(3)−O(3^a)	86.45(17)	Te(3)−O(4)−Te(1)	126.5(3)
O(4)−Te(3)−O(8^c)	88.26(16)	Te(2)−O(5)−Te(4^b)	111.6(3)
O(3^a)−Te(3)−O(8^c)	173.91(14)	Te(2)−O(6)−Te(1)	121.79(15)
O(9)−Te(4)−O(8)	100.95(21)	Te(4)−O(8)−Te(3^b)	117.8(3)
O(9)−Te(4)−O(2)	93.83(21)	Te(4)−O(9)−Te(2)	141.4(3)

^{a} $\bar{x}+1, \bar{y}+1, \bar{z}+1$. ^{b} $x, \bar{y}+1/2, z-1/2$. ^{c} $x, \bar{y}+1/2, z+1/2$. ^{d} $x+1, y, z$. ^{e} $x, y, z+1$. ^{f} $\bar{x}+2, \bar{y}+1, \bar{z}+1$. ^{g} $x-1, y, z$. ^{h} $x-1, \bar{y}+1/2, z+1/2$.

Table 5. Selected Bond Lengths (Å) in $K_2Te_2O_5$

Te(1)−Te(2)	3.7127(5)	K(1)−O(5)	2.6658(6)
Te(1)−Te(1^a)	3.7498(7)	K(1)−O(1^d)	2.7949(22)
Te(1)−Te(1^i)	3.8895(7)	K(1)−O(5^c)	2.798(5)
Te(2)−Te(2^b)	3.3898(3)	K(1)−O(3^b)	2.8034(22)
Te(1)−O(5)	1.8470(19)	K(1)−O(5^b)	2.856(5)
Te(1)−O(3)	1.858(5)	K(1)−O(2^k)	3.030(3)
Te(1)−O(4)	1.9146(21)	K(1)−O(2^d)	3.055(3)
Te(1)−O(3^a)	2.9064(22)	K(2)−O(4^b)	2.707(3)
Te(2)−O(1)	1.8335(16)	K(2)−O(5^e)	2.7350(23)
Te(2)−O(2^c)	1.914(3)	K(2)−O(1^c)	2.763(5)
Te(2)−O(2)	2.113(4)	K(2)−O(3^f)	2.7931(25)
Te(2)−O(4)	2.180(4)	K(2)−O(1^b)	2.814(5)
Te(2)−O(4^b)	2.9416(16)	K(2)−O(1^m)	2.8178(14)
K(1)−K(1^b)	3.4271(3)	K(2)−O(2^c)	3.0019(21)
K(1)−K(2^i)	3.7473(17)	K(2)−O(2)	3.2667(24)
K(1)−K(2^k)	3.7945(17)	Te(1)−K(1^c)	3.6140(12)
K(2)−K(2^l)	3.7489(21)	Te(1)−K(1^n)	3.7033(4)
O(1)−O(2)	2.763(4)	Te(1)−K(2^d)	3.8052(9)
O(1)−O(2^c)	2.815(3)	Te(1)−K(2^o)	3.8362(12)
O(2)−O(4^b)	2.679(3)	Te(2)−K(2^c)	3.5674(13)
O(2)−O(2^b)	2.7327(3)	Te(2)−K(1^e)	3.5797(9)
O(3)−O(4)	2.833(6)	Te(2)−K(2^b)	3.6939(12)
O(5)−O(4)	2.853(3)	Te(2)−K(2^o)	3.8313(5)

^{a} $\bar{x}, \bar{y}, \bar{z}$. ^{b} $x+1/2, \bar{y}+1/2, z$. ^{c} $x-1/2, \bar{y}+1/2, z$. ^{d} $x-1/2, \bar{y}, +1/2, z-1$. ^{e} $x+1/2, \bar{y}+1/2, z+1$. ^{f} $\bar{x}+1/2, y+1/2, \bar{z}+1$. ^{i} $\bar{x}+1, \bar{y}, \bar{z}$. ^{j} $x, y, z-1$. ^{k} $x-1, y, z-1$. ^{l} $\bar{x}+1, \bar{y}+1, \bar{z}+1$. ^{m} $\bar{x}+3/2, y+1/2, \bar{z}+1$. ^{n} $\bar{x}+1/2, y-1/2, \bar{z}$. ^{o} $\bar{x}+3/2, y+1/2, \bar{z}+1$.

Discussion

Structures Found in Tellurites. One of the key structural units of tellurites is the $TeO_{4/2}$ group, which is found in a distorted trigonal-bipyramidal conformation (Figure 1a).[11,12] Two of the bridging oxygens occupy axial sites on the tellurium atom, while the other two occupy equatorial sites. The lone pair of electrons occupies the third equatorial site, which results in distortion from the ideal trigonal-bipyramidal geometry: for example, the O_{ax}−Te−O_{ax} bond angle is typically 170° rather than the 180° of the undistorted form. The bond lengths of the axial and equatorial sites differ as well, with Te−O_{ax} typically 2.1 Å and Te−O_{eq} typically 1.9 Å. These units are found in both paratellurite (α-TeO_2),[11] and tellurite (β-TeO_2).[12] The linkages between the $TeO_{4/2}$ units confer rather different character to the different tellurites. Without exception, linked $TeO_{4/2}$ groups are bridged through the oxygen atoms such that an oxygen atom occupying an axial site on one tellurium will occupy an equatorial site on the linked tellurium and conversely (Figure 1f). Additionally, it is possible for two tellurium atoms to share two oxygen atoms, as in β-TeO_2, leading to so-called edge-shared groups (Figure 1g). Even in edge-shared groups, the O_{eq}−Te−O_{ax} alternation is maintained. All examples of the resulting four-membered rings we have found in Te^{IV} oxides are planar;[12,18−23] the rings typically show a parallelepiped shape,

(21) Daniel, F.; Moret, J.; Maurin, M.; Philipot, E. *Acta Crystallogr*. **1981**, *B37*, 1278.
(22) Andersen, L.; Moret, J. *Acta Crystallogr*. **1983**, *C39*, 143.

Table 6. Selected Bond Angles (deg) in $K_2Te_2O_5$

O(5)−Te(1)−O(3)	101.29(16)	Te(1)−O(4)−Te(2^c)	133.31(15)
O(5)−Te(1)−O(4)	98.66(8)	Te(2)−O(4)−Te(2^c)	81.42(4)
O(3)−Te(1)−O(4)	97.33(16)	O(5)−K(1)−O(1^d)	130.94(6)
O(1)−Te(2)−O(2^c)	97.39(12)	O(5)−K(1)−O(5^c)	99.49(13)
O(1)−Te(2)−O(2)	88.56(13)	O(5)−K(1)−O(3^b)	119.20(7)
O(1)−Te(2)−O(4)	91.12(14)	O(1^d)−K(1)−O(5^c)	93.50(11)
O(2^c)−Te(2)−O(2)	85.32(7)	O(1^d)−K(1)−O(3^b)	108.11(5)
O(2^c)−Te(2)−O(4)	81.47(14)	O(5^c)−K(1)−O(3^b)	88.73(12)
O(2)−Te(2)−O(4)	166.63(12)	O(4^b)−K(2)−O(5^e)	128.34(6)
Te(2)−O(1)−Te(1^g)	171.35(16)	O(4^b)−K(2)−O(1^c)	93.66(11)
Te(2^b)−O(2)−Te(2)	114.57(12)	O(4^b)−K(2)−O(3^f)	156.11(5)
Te(1)−O(3)−Te(1^a)	101.55(11)	O(5^e)−K(2)−O(1^c)	97.15(12)
Te(1)−O(3)−Te(2^h)	119.12(12)	O(5^e)−K(2)−O(3^f)	75.55(6)
Te(1^a)−O(3)−Te(2^h)	139.30(18)	O(1^e)−K(2)−O(3^f)	82.15(11)
Te(1)−O(4)−Te(2)	130.02(22)		

^{a} $\bar{x}$, $\bar{y}$, $\bar{z}$. ^{b} $x + 1/2$, $y + 1/2$, z. ^{c} $x - 1/2$, $\bar{y} + 1/2$, z. ^{d} $x - 1/2$, $\bar{y} + 1/2$, $z - 1$. ^{e} $x + 1/2$, $\bar{y} + 1/2$, $z + 1$. ^{f} $\bar{x} + 1/2$, $y + 1/2$, $\bar{z} + 1$. ^{g} $\bar{x} + 1$, $\bar{y}$, $\bar{z} + 1$. ^{h} $x - 1$, y, z.

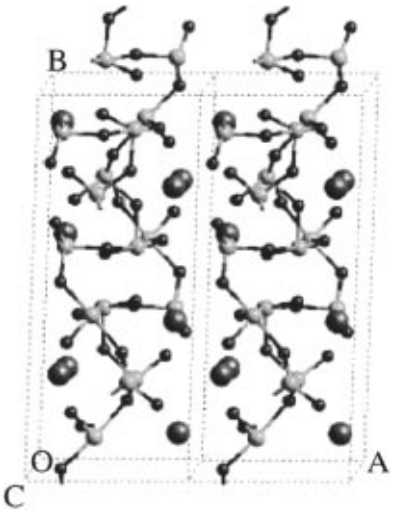

Figure 2. The structure of $K_2Te_4O_9$, shown in the crystalline *ab* plane. The isolated spheres are potassium cations, the light gray spheres linked with multiple bonds are tellurium, and the dark spheres are oxygen. This view shows two unit cells, separated by sheets of potassium cations. The 12-membered rings are visible in the center of each cell.

due to the bond length alternation and the deviation of the bond angles from 90°. In tellurite (β-TeO_2), all telluriums are members of edge-shared groups, resulting in a sheetlike structure of the solid. Paratellurite (α-TeO_2) contains no edge-shared groups, only corner-linked $TeO_{4/2}$. This solid has a rutile structure.[24] There are also examples of edge-shared groups in the Te^{VI} oxides,[25,26] one of which (Li_2TeO_4) is reported to be nonplanar.[27] Interestingly, the presence of edge-shared groups typically confers a faint yellow color of the associated crystals.[24]

While α-TeO_2 and β-TeO_2 represent the unmodified tellurites, the M_2TeO_3 compounds represent complete modification, in the sense that the tellurite network is fully cleaved. The M_2TeO_3 compounds are ionic solid and consist of TeO_3^{2-} groups (Figure 1e) coordinated by the alkali cations.[13−15] The TeO_3^{2-} ions represent the second main structural unit in the tellurites (the other being $TeO_{4/2}$): Te atoms coordinated to nonbridging oxygen (NBO). An oxygen bonded to a tellurium atom is termed an NBO if the distance to the next nearest tellurium

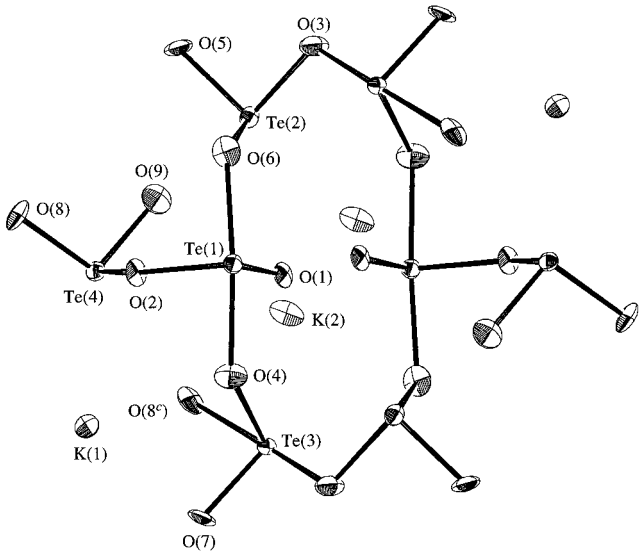

Figure 3. ORTEP diagram of $K_2Te_4O_9$, with thermal ellipsoids shown at the 90% probability level. The asymmetric unit is labeled (see Table 3 for symmetry operations). A second asymmetric unit, related to the first by inversion symmetry, is shown as well to illustrate how the 12-membered ring is formed. The four-membered ring, composed of secondary interactions, is located at the center of the 12-membered ring and connects Te(1), O(1), Te(1^a), and O(1^a).

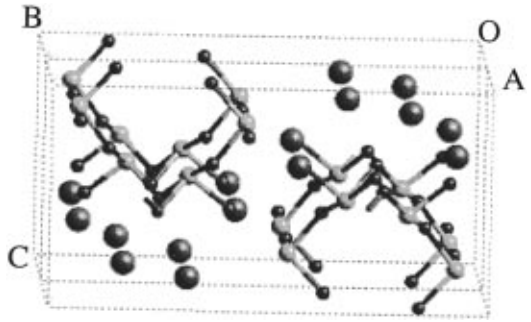

Figure 4. The structure of $K_2Te_2O_5$, looking down the crystal *a* axis. The structure consists of tellurite chains propagating down the *a* axis, interleaved by a rough sheet of potassium ions (shown as independent spheres). The tellurite chains are capped by nonbridging oxygens.

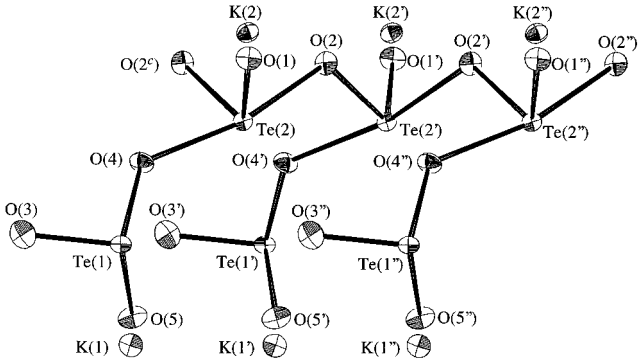

Figure 5. ORTEP diagram of $K_2Te_2O_5$, with thermal ellipsoids shown at the 90% probability level. The asymmetric unit is shown at the left, and two additional asymmetric units are shown as well, labeled with prime (′) and double prime(″). This shows how the tellurite chain grows, by linking Te(2) atoms through O(2).

atom is significantly longer than a Te−O bond; next-nearest distances for NBOs are typically on the order of 3.0 Å. The Te−NBO distance is shorter than other Te−O distances, typically being 1.84−1.88 Å. The TeO_3^{2-} ions can be described roughly as trigonal pyramidal, with the lone pair opposite the three oxygens. For K_2TeO_3[15] and Cs_2TeO_3,[17] the TeO_3^{2-} ions

(23) Johansson, G. *Acta Crystallogr*. **1978**, *B34*, 2830.
(24) Wells, A. F. *Structural Inorganic Chemistry*. Oxford University Press: Oxford, 1984.
(25) Kratochíl, B.; Jensovsky, L. *Acta Crystallogr*. **1977**, *B33*, 2596.
(26) Lindqvist, O.; Lundgren, G. *Acta Chem. Scand.* **1966**, *20*, 2138.
(27) Daniel, F.; Maurin, M.; Moret, J.; Philipot, E. *J. Solid State Chem*. **1977**, *22*, 385.

have C_{3v} symmetry, but in Li_2TeO_3 and Na_2TeO_3 the three Te−O bond lengths vary slightly.[13,14] The final important point, as far as network modification is concerned, is that in these compounds the number of NBOs is not equal to the charge on the ion (in contrast to Scheme 1 in the introduction). As discussed below, one or two units of charge distributed across two or three NBOs are stable and frequently occurring structures in modified tellurites. This behavior is quite different from simpler glass-forming oxides, such as SiO_2.

In the following sections, we will discuss the structures found in alkali tellurites as functions of the amount and type of added alkali oxide. Because Te−O bond lengths show a fairly wide dispersion, it is important to clearly identify the range of interactions that will be accepted as bonds. The sum of the ionic radii for Te^{IV} with a coordination number of 4, and O^{2-} with a coordination number of 2 is 2.01 Å,[28] and the sum of the covalent radii is 2.11 Å.[29] Typical Te^{IV}−O distances fall in the range from 1.8 to 2.2 Å, with a few examples extending beyond this. In the literature, contacts in the range from 2.6 to 2.7 Å have been called "weak bonding";[30] in a four-coordinate tellurium with such a long bond, however, the other three Te−O bond lengths are typically clustered tightly around 1.9 Å, as found in the TeO_3^{2-} ion. When the fourth bond is 2.3 Å or less, the remaining three bonds typically include two short distances (1.8−2.0 Å) and one intermediate distance (2.1 Å), which is more like the basic $TeO_{4/2}$ group described above. While Te−O contacts at 2.45 Å and greater may indeed arise from weak residual interactions, in this paper we will consider only contacts under 2.35 Å as full Te−O bonds.

Crystal Structures of Potassium Tellurites. Crystalline $K_2Te_4O_9$ is composed of infinite sheets of $[Te_4O_9]^{2-}{}_\infty$ in the *bc* plane surrounded by potassium cations (Figure 2). K(1) is coordinated to seven oxygen atoms, four of which are nonbridging. K(2) is coordinated to six oxygen atoms, three of which are nonbridging. In the asymmetric unit (Figure 4), each of the four tellurium atoms are bound to a single NBO, giving a total of four NBOs (O(1), O(5), O(7) and O(9)). Te(1), Te(2), and Te(3), along with their shared bridging oxygens, combine with their counterparts related by inversion symmetry to form a 12-membered ring (Figure 3). The center of inversion is at the center of the ring. These rings are bridged between Te(1) and Te(3) on neighboring rings through O(2), Te(4), and O(8). The chains of rings are weakly interconnected between Te(1) and Te(2) on adjacent rings through O(2), Te(4), and O(5). This linkage is weaker because Te(4)−O(5) is a secondary interaction (see below). The overall result is a sheet of 12-membered tellurite rings.

Of the four NBO atoms, three show possible secondary interactions (Te−O contacts at roughly 2.45 Å). The secondary interactions occur between Te(2) and O(9) at a distance of 2.4326(26) Å, between Te(1) and O(1^a) at a distance of 2.4890(4) Å, and between Te(4) and O(5^c) at a distance of 2.426(5)Å (Table 3). The first two of these secondary interactions yield additional rings in the structure. The six-membered rings completed by Te(2) and O(9) (or their counterparts related by inversion) are fused to the 12-membered ring. The secondary interactions between Te(1) and O(1^a) and their inversion-related counterparts form a four-membered, planar ring with angles similar to those seen in edge-shared units. The third secondary interaction, between Te(4) and O(5^c), involves the only tellurium atom not included in the 12-membered ring.

Table 7. Cation and Nonbridging Oxygen in Alkali Tellurite Crystals[a]

mol % of modifier	composition	M^+ CN	NBO/O	NBO/M^+	NBO/Te
0	α-TeO_2		0		0
	β-TeO_2		0		0
20	$Na_2Te_4O_9$	4, 5	0.22	1.0	0.5
	$K_2Te_4O_9$	6, 7	0.44	2.0	1.0
	$Cs_2Te_4O_9$	6, 7	0.44	2.0	1.0
33	α-$Li_2Te_2O_5$	3, 4	0.4	1.0	1.0
	β-$Li_2Te_2O_5$	3, 4	0.4	1.0	1.0
	$Na_4Te_4O_{10}$	5, 6	0.6	1.5	1.5
	$K_2Te_2O_5$	7, 7	0.6	1.5	1.5
	$Cs_2Te_2O_5$	6, 9	0.8	2.0	2.0
50	Li_2TeO_3	4, 4	1.0	1.5	3.0
	Na_2TeO_3	6, 6	1.0	1.5	3.0
	K_2TeO_3	6, 6, 6	1.0	1.5	3.0
	Cs_2TeO_3	6, 6, 6	1.0	1.5	3.0

[a] The first two columns give the crystal composition; the next column gives the coordination number of the alkali cations (multiple entries refer to crystallographically distinct sites); the final three columns give the number of nonbridging oxygens (NBO) per oxygen, modifier cation, and tellurium, respectively, per formula unit.

The tellurium sites in $K_2Te_4O_9$ show two types of binding: Te(1) and Te(3) are $TeO_{3/2}O^-$ sites (Figure 1b) and Te(2) and Te(4) are of the $TeO_{2/2}O$ type (Figure 1c). In these latter two sites, there are additional weak interactions to more distant oxygen atoms; discounting these interactions, the NBO in each site is best viewed as double-bonded to Te. If the secondary interactions were counted as bonding, Te(2) and Te(4) would also be of the $TeO_{3/2}O^-$ type.

The structure of crystalline $K_2Te_2O_5$ consists of infinite chains of $[Te_2O_5]^{2-}{}_\infty$ units running parallel to the *a* axis separated by corrugated sheets of potassium cations (Figures 4 and 5). The two potassium cations, K(1) and K(2), are each coordinated to seven oxygens, five of them nonbridging. The asymmetric unit contains three NBO atoms, O(1), O(3), and O(5), which leaves two bridging oxygen atoms linking the tellurium. The backbone of the infinite chains of $[Te_2O_5]^{2-}{}_\infty$ units is comprised of Te(2) and O(2). Te(2) (a $TeO_{3/2}O^-$ site) contains O(2) and O(4) in the axial positions and O(1), O(2^c), and the lone pair of electrons in the equatorial positions. O(1) is the only NBO that is bound to Te(2). Branching off the chains are the Te(1) groups, of the $TeO_{1/2}O_2^-$ type, which are linked to Te(2) through O(4).

Structural Comparison of Alkali Tellurites. Consideration of the alkali tellurite structures shows that modification proceeds roughly as shown in Scheme 1, insofar as introduction of alkali cations cleaves the tellurite network. There are significant differences from this simple view, however, and these differences are quantified in Table 7, which we now discuss in detail.

First, the coordination number of the alkali cations is not unity, as might be suggested by Scheme 1, but rather 3−9, increasing with the size of the cation (Table 7). This is because the NBOs do not dominate the coordination, although formally they carry the negative charge; the bridging oxygens participate just as much in cation coordination. We do not believe this point to be surprising, but it has been debated in the literature concerning glass-forming oxides.[31−33] The coordination numbers do not show any particular trend as the extent of modification is increased.

Secondly, the coordination number of tellurium decreases with modification from 4 to 3. By the 50% modification level, all Te atoms are three−coordinate, but these sites appeared

(28) Shannon, R. D. *Acta Crystallogr*. **1976**, *A32*, 751.
(29) Shriver, D. F.; Atkins, P. W.; Langford, C. H. *Inorganic Chemistry*; W. H. Freeman: New York, 1990.
(30) Hanke, K.; Kupcik, V.; Lindqvist, O. *Acta Crystallogr*. **1973**, *B29*, 963.
(31) Zhang, M.; Boolchand, P. *Science* **1994**, *266*, 1355.
(32) Zwanziger, J. W.; Tagg, S. L.; Huffman, J. C. *Science* **1995**, *268*, 1510.
(33) Zhang, M.; Boolchand, P. *Science* **1995**, *268*, 1510.

Table 8. Tellurite Structures Found in Different Alkali Tellurite Crystals

mol % of modifier	composition	$TeO_{4/2}$	$Te_{3/2}O^-$	$TeO_{2/2}O$	$TeO_{1/2}O_2^-$	TeO_3^{2-}
0	α-TeO_2	1				
	β-TeO_2	1				
20	$Na_2Te_4O_9$	1	2	1		
	$K_2Te_4O_9$		2	2		
	$Cs_2Te_4O_9$		2	2		
33	α-$Li_2Te_2O_5$		2			
	β-$Li_2Te_2O_5$		2			
	$Na_4Te_4O_{10}$		1		1	
	$K_2Te_2O_5$		1		1	
	$Cs_2Te_2O_5$				2	
50	Li_2TeO_3					1
	Na_2TeO_3					1
	K_2TeO_3					1
	Cs_2TeO_3					1

already at the 20% modification level ($Na_2Te_4O_9$ and $K_2Te_4O_9$). This indicates the most significant departure in this system from the simple chemistry of Scheme 1. In Scheme 1, the Si atoms always remain four−coordinate, as is also the case in P_2O_5 materials. Well-studied non-oxide chalcogenides, like Ge−Se and As−S solids, retain a similarly close relationship between oxidation number and coordination number, which has led, in our view, to an over-reliance on the so-called $8 - N$ rule to describe bonding in main-group glass-forming materials.[31,34] In the tellurites, as in the borates, this rule does not apply; it also fails to apply to coordination of the alkali cations.

Columns 4−6 of Table 7 show the increase in NBO units as a function of modifier content and concomitantly the decrease in $TeO_{4/2}$ groups. Note that the number of NBOs depends on the modifier ion used: for a given composition, the largest cation induces the largest NBO fraction, until the 50% modification level where 1 equiv of modifier ions induces 1.5 equiv of NBOs. Unlike the simpler case of silicates, the number of NBOs is observed to exceed, in most cases, the number of added modifier ions. This occurs because of the stability of multiple NBOs on a common Te atom sharing a single delocalized charge. At the 20% modification level, K^+ and Cs^+ induce twice as many NBOs as Na^+, and at 33%, Cs^+ induces 2.0 NBOs each, Na^+ and K^+ induce 1.5 NBOs each, and Li^+ induces only 1 NBO.

The observation that larger cations induce more NBO formation correlates with the trend in cation coordination number in this system. We believe that these trends are connected and are due to the bulkiness of anions formed in this system. As noted, the tellurites tend toward large anions, in which two or three NBOs stabilize one or two negative charges, respectively, ultimately creating TeO_3^{2-} anions at the 50% modification level. The tellurite groups formed in the different compounds are detailed in Table 8. At the 20% modification level, $Na_2Te_4O_9$, $K_2Te_4O_9$, and $Cs_2Te_4O_9$ contain $TeO_{3/2}O^-$ groups, which are the analogs of the structures shown in Scheme 1 (the potassium and cesium compounds contain twice as many as expected, based on the amount of added modifier, however). They also contain $TeO_{2/2}O$, which includes a double-bonded oxygen, as found in phosphates but not silicates. At the 33% level, the Li solids contain only the $TeO_{3/2}O^-$ groups while the Na, K, and Cs solids contain these groups and also $TeO_{1/2}O_2^-$ groups. The latter are bulky units in which one negative charge is delocalized over two NBOs; no analog for such structures exists in the silicates (Scheme 1). These units are considerably harder to pack around a small cation than are singly charged NBOs, as found in silicates, and moreover, this steric constraint will be relaxed for larger cations. Thus, we rationalize the NBO formation increase with increasing cation size as arising from the lower energy cost of packing large ions around larger cations, as compared to the high cost of packing such species around small ions like lithium.

Finally, we note that edge-shared units occur in some of the structures, notably the sodium compounds at 20% and 33% modification and β-$Li_2Te_2O_5$.[18−20] The 20% modified potassium compound contains a remnant of edge-shared groups, completed as noted above through secondary interactions between Te(1) and O(1). The cesium compounds contain no edge-shared groups.

Conclusions

We have reported the structures of $K_2Te_4O_9$ and $K_2Te_2O_5$, completing the series of structures of Li, Na, K, and Cs tellurites up to 50% added alkali oxide. The new structures show that while potassium acts like a conventional modifier in the sense of inducing nonbridging oxygen, it does so at a significantly higher rate than do the lighter alkali oxides. In fact, each composition (below 50% modification) shows a trend of increased NBO formation with increased size of the modifier. We ascribe this trend to the tendency in this system toward bulky anionic groups in which negative charge is delocalized across several NBOs. These groups form in greater abundance in the heavier alkali tellurites, and our explanation is that these groups pack more easily around the larger, more highly coordinated cations like potassium and cesium, in contrast to small ions such as lithium. Finally, edge-shared groups, which are common in the sodium compounds, appear in one of the lithium structures but not in the other modified compositions.

We are currently in the process of using these insights from the alkali tellurite crystal structures to interpret NMR, Raman, and neutron-diffraction data obtained on glasses in the same range of compositions.

Acknowledgment. It is a pleasure to thank Dr. Ulrike Werner-Zwanziger for helpful discussions. This research was supported by the National Science Foundation (Grant No. DMR-9508625).

Supporting Information Available: Tables of atomic data, crystal data, data collection and refinement, fractional coordinates, and anistotropic thermal parameters for $K_2Te_4O_9$ and $K_2Te_2O_5$ (7 pages). Ordering information is given on any current masthead page. Structure factors are available from the authors on request.

IC970497M

(34) Mott, N. F.; Davis, E. A. *Electronic Processes in Non-Crystalline Materials*; Oxford University Press: Oxford, 1979.